Magnetic characterization of Fe and Fe-Phosphate particles

Author: Kirnjeet Kaur
Advisors: Dr. Javier Tejada Palacios and Jaume Calvo de la Rosa
Facultat de Física, Universitat de Barcelona, Diagonal 645, 08028 Barcelona, Spain.*

Abstract: In this work, the magnetic properties of one Soft Magnetic Material (SMM) and one Soft Magnetic Composite (SMC) are studied as a function of different particle size distribution. X-Ray Diffraction (XRD) show that both samples consist on an iron core. The basic magnetic characterization of the samples is done by measuring the isothermal magnetization M(H) curves and zero field cool (ZFC) – field cool (FC) curves. The results show that, despite being magnetic iron particles, they present an extremely narrow hysteresis loop. Moreover, it has been seen that the higher the size distribution is, the greater the magnetic saturation is achieved. In order to study them from the point of view with more technological and industrial interest, their functional properties are measured in a wide frequency range. In this regard, Impedance Spectroscopy is used to measure their magnetic permeability between 1 kHz and 13 MHz while their dielectric constant is studied from 200 MHz to 20 GHz by using a Pulse Network Analyser (PNA). Finally, reflection loss measurements are performed in order to measure directly the energy absorbed in the range between 7 GHz and 10 GHz.

INTRODUCTION

Soft Magnetic Materials (SMM) are ferromagnetic or ferrimagnetic materials which magnetize and demagnetize very easily because of a strong magnetic moment. These materials are characterized by a high permeability, small hysteresis loss and high saturation magnetization. Pure iron powders, steel or soft ferrites are some of the examples of SMM. Despite having small magnetic losses due to a narrow hysteresis loop, Eddy currents losses are quite high because of a low electrical resistivity [1]. In order to solve this problem, a new generation of materials called Soft Magnetic Composites (SMC) is getting attention from last years. These materials are basically made by SMM core covered with an insulating shell, which increases the electrical resistivity between particles. They exhibit several worthy advantages when particle size, shape and microstructure are optimized [2]. The latest developments of SMC have led to materials with significantly increased performance such as lower losses, higher permeability, increased mechanical strength and higher electric resistivity [3], which make them very useful when working with alternating magnetic field [4].

On the one hand, all these properties can be beneficial from the view of technological applications, for example, in the manufacturing of electrical machines. For instance, stacked laminated steel sheets, separated by an insulator, have been used in the making of electric motors and other alternating current devices for more than a century [5]. When working with alternating current, steel or iron present important Eddy current losses as the frequency is increased. This is where SMC can be of great use. Since particles are covered with insulating coatings, losses due to Eddy currents, and hence heat effects, are drastically reduced [6].

On the other hand, permeability and magnetic saturation are seen affected by the thickness of the coating, which mean that an optimal amount of insulation should be used in order to maximize these properties [6]. In direct current applications, low electric resistivity is required but because of the insulation layer, electric resistivity becomes higher. In this case, SMC suffer a disadvantage [5]. So, the future of SMC lies in finding materials which exhibit the highest permeability, low coercivities, a high magnetic induction, coupled with a coating material that allows the lowest core losses obtained by high electrical resistivity and good magnetic capabilities [2]. Such materials open up possible benefits like low-cost and low-waste production and usage of less amount of material which leads to a size and weight reduction [6].

The aim of the present work is to analyse and compare the magnetic properties of a SMM powder and a SMC one, and discuss the effect that the insulating coating has on final properties. Each sample is subdivided by its particle size distribution. The notation used for each sample is summarized in table 1.

Size distribution (in μm)	**Notation**	
	SMC	**SMM**
45 – 106	SMC_045_106	SMM_045_106
106 – 160	SMC_106_160	SMM_106_160
160 – 999	SMC_160_999	SMM_160_999
All sizes	SMC	SMM

Table 1: Notation used to describe all the samples. "SMC all sizes" distribution is centred at 200 μm and 100 μm in case of SMM.

Many properties like permittivity, permeability, reflection loss, etc. depend strongly on the frequency range. In most textbooks, they are shown as a constant value which is only true in the lower frequency range. In this project, all these properties are investigated in an extensive range of frequencies and their dependency on particle size distribution is discussed.

THEORETICAL AND EXPERIMENTAL FRAMEWORK

The study of these samples is subdivided into five different parts.

A) Sample identification

XRD measurements are performed for the identification of the two samples using *PANalytical X'Pert PRO MPD θ/θ Bragg-Brentano powder diffractometer of 240 millimetres of radius with Cu Kα radiation*. *X'Pert HighScore Software*

* Electronic address: kkaurkau7@alumnes.ub.edu

is used to do the peak analysis and verify that they are made of iron. Furthermore, images are taken with the help of a Scanning Electronic Microscope (SEM), named as *Electronic Microscope 200 FEI, XTE 325/D8395*, which show any possible morphology differences between these two, such as the insulating layer on the top of the SMC sample.

B) DC Magnetic characterization

The magnetic behaviour of all samples is studied as a function of applied magnetic field (M(H) curves) and temperature (ZFC – FC curves) with the help of a SQUID-magnetometer (Superconducting Quantum Interference Device). M(H) measurements are done by applying magnetic field between -15000 Oe and 15000 Oe at room temperature using a very small amount of the sample (less than a mg) as they have a strong magnetic moment, so, they magnetize very easily. To obtain the ZFC curve, the temperature is decreased to very low values with H = 0 and then, increased to room temperature with H = 5000 Oe. From this point, the temperature is decreased again with the same magnetic field to obtain the FC curve.

C) Permeability

Permeability is a complex and frequency-dependent magnitude, the real part indicates the energy storage/release mechanisms and the imaginary part represents the loss effect.

Complex permeability spectra is measured with an impedance analyzer (HP 4192 A) from 1 kHz to 13 MHz with the contact electrodes in two-terminal connection configuration. The measurements are carried out with the sample compacted into a toroidal- shaped core wrapped with an insulated wire whose interior radius (R_{in}) is of 3.6 mm and the exterior radius (R_{out}) is 6.9 mm. From the impedance analyzer device, values of impedance (Z), frequency (ω) and phase (θ) are obtained which are related to the permeability by the following equations.

$$Z_C = (|Z|\cos\theta - R_o) + i\,|Z|\sin\theta \qquad (1)$$

where Z_C is the sample impedance calculated from the complex impedance, Z, the system assembly's resistance, R_o (experimental value), and the phase, θ.

$$Z_b = (Z_C - i\omega C_P)^{-1} = Z_b' + iZ_b'' \qquad (2)$$

C_P is the parasitic capacitance of the device which can be deduced by fitting the experimental data with the well known Davison-Cole model (DC model). The real (μ_r') and the imaginary (μ_r'') permittivity can be written in terms of Z_b, ω and L_o. L_o is the inductance of the toroidal-shaped sample which depends on its physical parameters.

$$L_o = \frac{\mu_o N^2 h \ln(r_{out}/r_{in})}{2\pi} \qquad (3)$$

where N is the number of wire turns around the toroid, μ_o is the vacuum permeability and (h, r_{out}, r_{in}) are toroid's dimensions, h being its height and r, the radius.

$$\mu_r'(\omega) = \frac{Z_b''}{\omega L_o} \;\; ; \;\; \mu_r''(\omega) = \frac{Z_b'}{\omega L_o} \qquad (4)$$

As mentioned before, by fitting the experimental data with the DC model, some interesting properties like permeability relaxation time and the relaxation behaviour can be found, which will be discussed below.

Davison-Cole model

The relaxation model proposed by Debye is an ideal case where an instantaneous relaxation of the material is assumed at a certain frequency, which means there is a single relaxation time (τ). But this is not the case with real materials as τ is affected by the particle size distribution, which is why there is a distribution of τ. In these cases, Davison-Cole model is more accurate and a generalized method. It works with four parameters, μ_r^s (μ_r' at the lowest frequency), μ_r^∞ (μ_r' at the highest frequency), τ (characteristic relaxation time) and n. The n parameter is a real number between 0 and 1 which indicates whether there is or not a distribution of τ, zero being an ideal case with one relaxation time. Equations (5) and (6) describe the complex permeability according to the DC model [7]. For the data treatment, a self-made Python code is used and all four parameters are found in a given error range.

$$\mu_r' = \mu_r^\infty + \frac{\mu_r^s - \mu_r^\infty}{[1 + (\omega\tau)^2]^{\frac{1-n}{2}}}\cos[(1-n)\arctan(\omega\tau)] \qquad (5)$$

$$\mu_r' = \frac{\mu_r^s - \mu_r^\infty}{[1 + (\omega\tau)^2]^{\frac{1-n}{2}}}\sin[(1-n)\arctan(\omega\tau)] \qquad (6)$$

D) Permittivity

Just like permeability, permittivity is also complex and it describes the ability of the material to store and release electromagnetic energy in the form of electric charge and it depends on the frequency of the applied electric field (**E**). For higher values of frequency, a material's polarization is not able to follow the rapid changes of the **E** and this time-lag between these two magnitudes can be represented by a phase difference. For this reason, permittivity is treated as a complex property [8].

In this project, permittivity measurements are performed in the frequency range of 200 MHz to 20 GHz with *HP 8517B S-Parameter Test Set* device which is previously calibrated by using *85070C Dielectric Probe Kit*. The "S-parameter" used is S_{11} which means that the microwave signal comes out from the port 1 and immerses into the sample. A part of this signal is reflected, which goes back through the port 1. The complex permittivity is determined by these incident and reflected signals and the geometry of the detector by the device.

Since samples are in the form of powders, the amount of air present inside them may have a major impact on the measurements. To determine the air effect, five measurements are made for each sample by changing the pressure applied on them. After that, all the experiments are repeated using two different volumes (5 ml and 10 ml) to verify any possible differences due to the amount of the sample used.

To complement the results obtained from the previous experiments, cylindrical shaped discs of 4 mm

(approximately) in thickness and 2.8 mm in diameter are made by compressing a few grams of the sample (~ 4 g) under 700 kg/cm^2 of pressure. A higher permittivity is expected in the case of SMM samples, as they are pure iron particles, and the cylindrical discs because no air is present in them unlike the powder samples.

E) Reflection loss

When an electromagnetic wave propagates through a material, it can be reflected (R), transmitted (T) or absorbed (A) by the material, A+R+T = 1. To determine which of the two samples, SMM or SMC, present more reflection losses, a PNA Series Network Analyser (E8361A) is used to perform measurements in the range of 7 – 10 GHz. PNA is connected with a completely metallic cavity which encloses the sample, which implies that T = 0. A microwave signal is sent from the port 1 which goes through the sample and it is reflected back to the port 1 (S_{11} parameter). The difference between these signals is used to find the reflection losses as a function of frequency.

RESULTS AND DISCUSSION

A) Sample identification

XRD technique is performed for the identification of the two samples and by doing peak analysis, they are identified as cubic iron (Reference code: 00-006-0696).

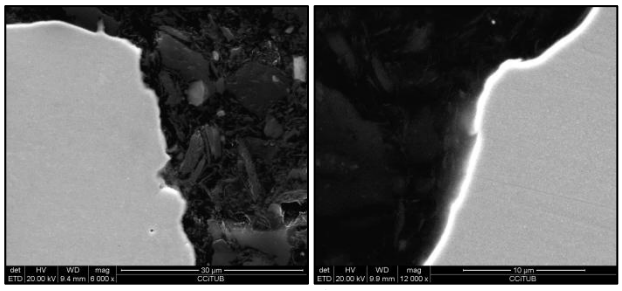

Figure 1: Images taken by SEM. SMM (left) and SMC (right)

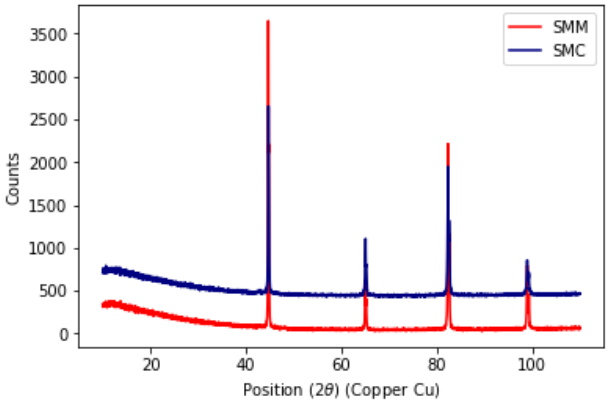

Figure 2: XRD pattern of SMM and SMC samples. In case of SMC sample, a constant number of 400 counts has been added for a better visibility.

Regarding the SMC sample, images taken by the SEM highlight the coating of each iron particle demonstrating its isolating behaviour as it retains electrons (Figure 1). Since XRD pattern for both the samples is identical (Figure 2), any possible differences in their magnetic behaviour may be due to the coating. Furthermore, the coating of the SMC sample has been identified with a phosphate by using the Fourier Transform Infrared Spectroscopy (FT-IR) [9].

B) DC magnetic characterization

Figure 3 represents the first magnetization curve for each sample measured at room temperature. The magnetization is higher in the case of iron particles (SMM) and it increases with the size of the sample particles. *SMC_106_160* presents a different tendency, which we assume that is due to the uncertainty in the measurement of its mass as the mass used is of the same order of magnitude as the last decimal digit of the weighting scale.

It has been seen that these materials present a very narrow hysteresis loop. Experiments have shown that these curves are very unique for each sample, neither they depend on the temperature nor the frequency we change the field (G/s). A large spectrum of frequencies has been covered (approximately between10^2 G/s and 10^8 G/s) but the same results have been found. This is a surprising fact as both samples are iron-based.

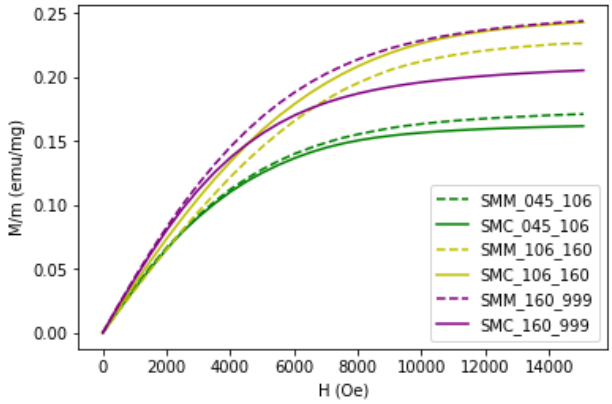

Figure 3: Magnetization versus magnetic field curves for different size samples at 300 K. SMM (discontinuous line) and SMC (continuous line)

Alongside with M(H) curves, ZFC-FC curves are obtained by measuring magnetization as a function of temperature when a magnetic field of 5000 Oe is applied.

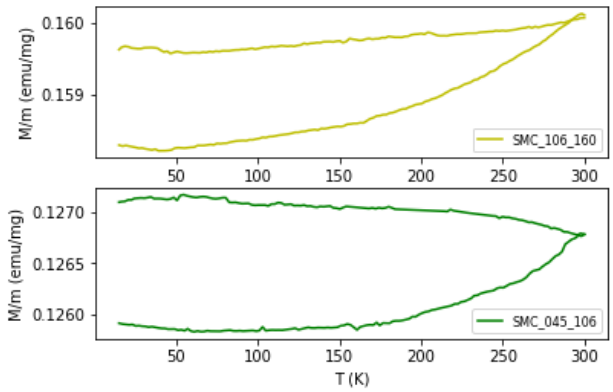

Figure 4: ZFC-FC curves of SMC sample obtained by applying H = 5000 Oe.

For both the samples, typical ZFC-FC curves for ferromagnetic materials can be seen which indicate a

blocking temperature higher than 300 K (Figure 4). The fact that these materials do not have a remanent magnetization, but they do present irreversibility in ZFC-FC curves seems almost contradictory. Studies are being done to find out an explanation of this behaviour.

C) Permeability

Equations [1 – 4] are used to find the experimental complex permeability and then, equations [5 – 6] are used to fit the experimental data to the DC model. All the data is treated with the help of a self-made Python code and results obtained are presented in the table 2.

Sample	**SMM**	**045_106**	**106_160**	**160_999**
μ_r^s	101.89	114.64	108.60	165.25
μ_r^∞	1.23	1.06	1.00	1.02
C_p (10^{-10}) J·K^{-1}	0.95	0.77	3.20	0.54
n	0.46	0.44	0.41	0.41
τ (10^{-6} s)	2.75	1.87	1.55	5.00
N	15	14	15	14
R_0 (Ω)	0.039	0.035	0.039	0.038
h (mm)	3.6	3.1	3.4	2.2
Sample	**SMC**	**045_106**	**106_160**	**160_999**
μ_r^s	67.38	61.89	81.64	84.24
μ_r^∞	1.35	1.00	1.19	1.00
C_p (10^{-10}) J·K^{-1}	0.089	0.128	0.110	1.000
n	0.60	0.61	0.54	0.42
τ (10^{-6} s)	0.295	0.322	1.515	0.570
N	15	15	16	15
R_0 (Ω)	0.042	0.046	0.040	0.040
h (mm)	4.7	3.9	3.8	4.3

Table 2: Different parameters obtained by fitting the experimental data to the DC model. N, R_0 and h are experimental values.

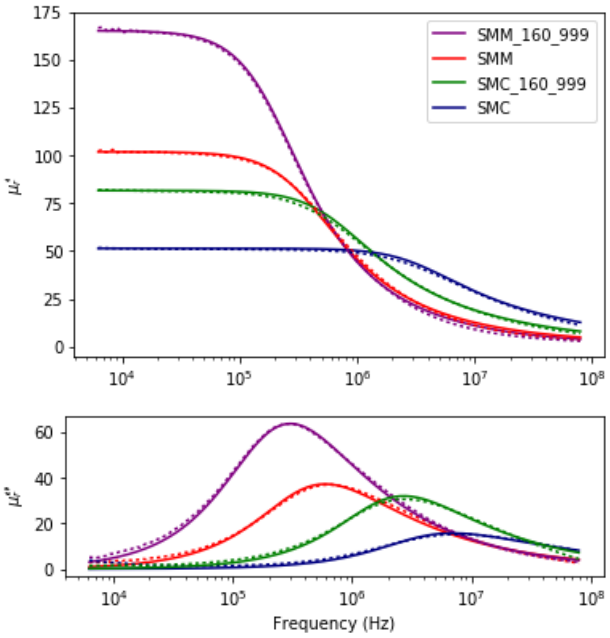

Figure 5: Experimental real permeability (μ_r') and imaginary permeability (μ_r'') data (dotted lines) and DC model fit (continuous lines).

The static permeability (μ_r^s) is greater in the case of SMM sample and, in general, it increases with particle size distribution. Experimental data indicates the sample with a higher static permeability has a lower relaxation frequency, which means that the material losses its permeability faster as the frequency is increased. This phenomenon can be seen in Figure 5 where the real permeability starts decreasing with an increase in the imaginary part. The τ is inversely proportional to the relaxation frequency. So, the smaller the relaxation frequency is, the greater the relaxation time is. From the point of view of high frequency technological applications, materials with smaller values of relaxation frequencies should be avoided.

Since the n-parameter is greater than zero, the relaxation model follows the DC model and there is a continuous distribution of relaxation times. Figure 6 represents the imaginary permeability as function of real permeability (Cole-Cole diagram). The Cole-Cole diagram of materials that follow Debye's model is a semi-circle.

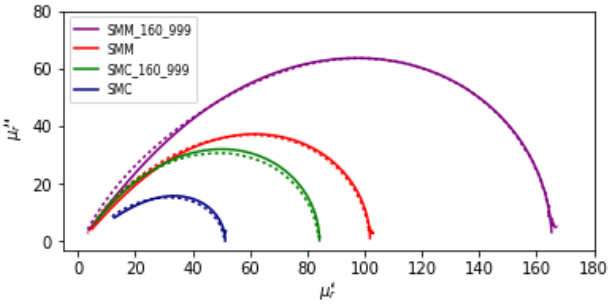

Figura 6: Cole-Cole diagram of SMM and SMC samples. Experimental data is represented by the dotted line and the DC model fit data is the continuous line.

D) Permittivity

As mentioned in the previous section, complex permittivity is measured between 200 MHz and 20 GHz. Experimental data shows that the permittivity not only increases with the amount of pressure applied on the sample but also with the quantity of the sample used to do the experiment. The real permittivity is the highest when applied the maximum pressure for 10 ml of the sample. This observation is intuitive as by applying higher pressures, air is eliminated.

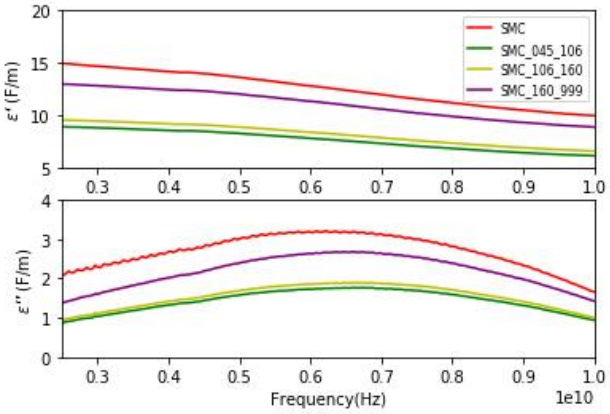

Figure 7: Real permittivity (ε') and imaginary permittivity (ε'') as a function of frequency for SMC particles.

As shown in Figure 7, there is a clear increase in the permittivity as the particle size gets bigger. The same behaviour is observed for different volumes, pressures

and samples with very few exceptions which could be associated with a bad calibration. It is worth mentioning here that the device used to do the measurements is very sensible to the calibration. Two different calibrations can lead to different numerical values of permeability. Experiments done with the compacted cylindrical discs are also seen affected by the calibration. In general, they present a higher permittivity than the powders but no clear tendency is observed.

E) Reflection losses

The data obtained by the Pulse Network Analyser (PNA) is smoothed by averaging over 50 points and the smoothed data is represented as a function of frequency in the Figure 8. The y-axis represents the difference between the intensities of the incident and the reflected wave.

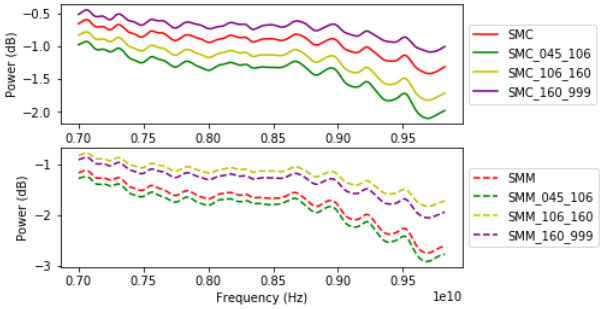

Figure 8: Reflexion loss smoothed experimental data as a function of frequency.

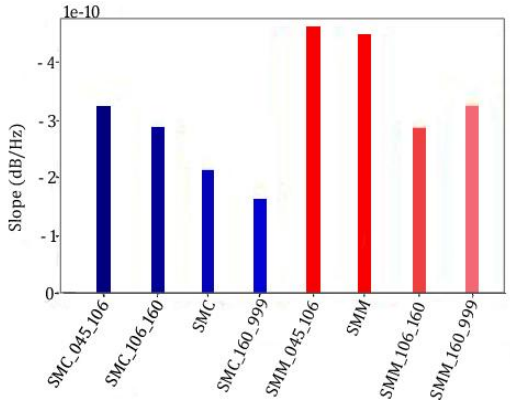

Figure 9: Slope of the smoothed Power(frequency) curves of SMM and SMC samples.

Results show that SMM sample absorbs more than the SMC sample and the absorption increases with frequency. SMC sample reflects more and the reflection decreases, hence the absorption increases, with the frequency.

In general, smaller size particles absorb more than the bigger size particles. Figure 9 represents the slope of the smoothed Power (frequency) curves (Figure 8) obtained by doing a lineal regression. Smaller size particles have a higher slope which means that their absorption rate is higher.

CONCLUSIONS

The first magnetization curves of the samples have shown a higher magnetic saturation for SMM which increases with the particle size distribution. Despite having irreversible ZFC-FC curves with a blocking temperature above 300 K, both materials present a very narrow hysteresis loop.

The study of the magnetic permeability has indicated an increase in the real permeability with the particle size distribution. SMM have a higher permeability and a lower relaxation frequency in all cases. So, in the low range of frequencies, SMM with big size particles are a great option as their static permeability is higher. But for high frequency applications, SMC will perform better than SMM as their relaxation frequency is higher. Furthermore, permittivity measurements have shown an important dependence on the volume of the sample, the presence of the air molecules and the particle size distribution. An increasing tendency with particle size distribution has been observed. Finally, experiments done with PNA in the range of 7 – 10 GHz have indicated an increase in the absorption rate with frequency with SMC being more reflexive than SMM.

Acknowledgments

I would like to express my sincere gratitude to my advisors Dr. Javier Tejada and Jaume Calvo for their complete guidance and wonderful advices throughout the project. I want to thank my dear friend Alba Teixidó who has participated in all the experiments, data analysis and discussions. It has been a great experience working with all of them. I am also grateful to Dr. J.M. Hernández and Chao Chen for helping us in the laboratory.

[1] F. Fiorillo, C. Appino & M. Pasquale. "Soft Magnetic Materials". Wiley Encyclopedia of Electrical & Electronics Engineering, [Online]. DOI: 10.1002/047134608X.W4504.pub2 (2016)

[2] Katie Jo Sunday and Mitra L. Taheri. "Soft magnetic composites: recent advancements in the technology". *Metal Powder Report* Volume 72, Number 6. Department of Materials Science and Engineering, Drexel University, Philadelphia, PA, United States (2017)

[3] "SMC developments boost performance and strength". *Metal Power Report*. July/August 2010.

[4] Andreas Boehm and Ingo Hahn. "Comparison of Soft Magnetic Composites (SMCs) and electrical steel". IEEE.

[5] "Seeking a different path to 3-D SMC electric motors". *Metal Power Report*. November/December 2009.

[6] P. Kollár, Z. Birčáková, J. Füzer, R. Burěs, M. Fáberová. "Power loss separation in Fe-based composite materials". *Journal of Magnetism and Magnetic Materials* **327**, 146–150 (2013).

[7] C. Chao. "High frequency properties of micrometer magnetic particles". Treball de fi de grau, Universitat de Barcelona (2018).

[8] Nigel J. Cassidy, Ground Penetrating Radar Theory and Applications. Chapter 2, Electrical and magnetic properties of rocks, soils and fluids. UK: Elsevier B.V. Pages 44-57. (2009)

[9] J. Urtasun. "Magnetic Characterization of SMCs". Treball de fi de grau, Universitat de Barcelona (2017).